

These spectral features and behavior are entirely consistent with a monodentate, N7-coordinated 5'-AMP with the 5'-PO<sub>4</sub> group limited to an outer-sphere role.<sup>11</sup> Direct phosphate coordination, as observed for Rh(III)-inorganic phosphate or Rh(III)-methyl phosphate, causes downfield shifts of 8-10 ppm in <sup>31</sup>P spectra.<sup>14,15</sup> However, this outer-sphere interaction appears to be crucial, since it facilitates coordination of N7. Inspection of plastic or graphic models of [Rh(tren)(H<sub>2</sub>O)(5'-AMP-N7)]<sup>+</sup> (I-5'-AMP) reveals that the 5'-PO<sub>4</sub> is ideally positioned for H bonding with the tren and H<sub>2</sub>O ligands (Figure 2).

Further evidence for the outer-sphere role of the 5'-PO<sub>4</sub> group in the formation of I-5'-AMP is found in the absence of N7 coordination in the Rh(tren) complexes formed with both 3'- and 2'-AMP. For complexes of these nucleotides, the <sup>1</sup>H signal did not shift significantly; the principal spectral change was a 7-10 ppm downfield shift of the <sup>31</sup>P NMR signal, indicative of phosphate group coordination. The position of the phosphate groups of these nucleotides is not correct for an outer-sphere role in promoting N7 coordination as illustrated for the hypothetical N7-bound 3'-AMP in Figure 2.

As expected from the Guo results, 5'-GMP initially forms an analogous N7-bound complex, I-5'-GMP (*t*<sub>1/2</sub> ~ 1 h). However, after 24 h, this species converted into a second complex II-5'-GMP (*t*<sub>1/2</sub> ~ 5 h). The chemical shift of the H8 signal of this species at 8.41 ppm can be compared with values of 8.89 ppm for I-5'-GMP and 8.14 ppm for 5'-GMP, respectively. The H1' signal is a doublet at 5.93 ppm for I-5'-GMP and at 5.88 ppm for 5'-GMP, but a singlet at 6.02 ppm for II-5'-GMP. Furthermore, the H2' signal has shifted downfield to 5.2 ppm from 4.8 ppm in the free nucleotide. This pattern of shifts is characteristic of an N<sup>7</sup>,5'-PO<sub>4</sub> chelate.<sup>9-12</sup> Distortion of the sugar ring into an N pucker (*J*<sub>H1'-H2'</sub> ~ 0) accounts for the singlet, and the placement of H2' in the guanine base deshielding region accounts for the downfield shift.<sup>12</sup> The same behavior was observed for 5'-IMP and 5'-dGMP. The <sup>31</sup>P signals for these complexes have shifted downfield by 5-7 ppm, a shift also consistent with chelation. We conclude that I-5'-GMP and II-5'-GMP are [Rh(tren)(H<sub>2</sub>O)-(5'-GMP-N7)]<sup>+</sup> and [Rh(tren)(H<sub>2</sub>O)(5'-GMP-N<sup>7</sup>,5'-PO<sub>4</sub>)]<sup>+</sup>, respectively.

I-5'-AMP and I-5'-dAMP also convert to second species, II-5'-AMP and II-5'-dAMP (*t*<sub>1/2</sub> ~ 24 h and 20 h, respectively), with some spectral characteristics of an N<sup>7</sup>,5'-PO<sub>4</sub> chelate (H8 at 8.55 ppm, *J*<sub>H1'-H2'</sub> = 4.4 Hz, and H1' at 5.88 ppm for 5'-AMP; H8 at 8.43 ppm, *J*<sub>H1'-H2'</sub> = 5.6 Hz, and H1' at 6.23 ppm for 5'-dAMP; 5-6 ppm downfield shift of the <sup>31</sup>P signal). In the only reported 5'-dAMP N<sup>7</sup>,5'-PO<sub>4</sub> chelate, [Cp<sub>2</sub>Mo(5'-dAMP-N<sup>7</sup>,5'-PO<sub>4</sub>)], *J*<sub>H1'-H2'</sub> is 4.6 Hz.<sup>13</sup> The reason for this difference between 5'-AMP and 5'-GMP chelates, including the absence of a large downfield shift of the H2' signal for 5'-AMP, is not clear.

One problem encountered when Ado and 5'-AMP reactions are followed by <sup>1</sup>H NMR is the relatively fast rate of H8 exchange in D<sub>2</sub>O. After 24 h at 60 °C, ~70% of the original H8 signal has been lost. To follow changes in the H8 peak, the reactions were also carried out in H<sub>2</sub>O.<sup>16</sup> The fast formation (*t*<sub>1/2</sub> < 2 h) of I-5'-AMP, followed by slow conversion to a second complex, was confirmed.

The role that the phosphate group plays in directing the attack of a metal center on a nucleobase has been the subject of speculation.<sup>7,17</sup> Our results demonstrate that a 5'-phosphate can direct nucleobase coordination. Qualitative molecular modelling with unperturbed B-DNA suggests that H-bond donor ligands equatorial to the axial attack direction could form H bonds to phosphate

oxygens. The role such interactions may play in the attack of Pt(II) anticancer drugs on DNA<sup>17,18</sup> merits investigation. Unlike our Rh(III) results, the Pt(II) drugs readily form adducts with both Ado and 5'-AMP,<sup>11</sup> and therefore the outer-sphere role of the phosphate group is difficult to detect experimentally. The clear demonstration of the formation of an N<sup>7</sup>,5'-PO<sub>4</sub> chelate with a fourth metal center, Rh(III), in addition to recently discovered examples with Pt(II),<sup>10,11</sup> Ru(II),<sup>12</sup> and Mo(IV),<sup>13</sup> in the short time since the initial recognition of the characteristics of such species in 1986<sup>10</sup> argues that such chelates may indeed be ubiquitous, although elusive, species in metal nucleotide chemistry.

**Acknowledgment.** We thank the National Science Foundation for a Visiting Professorship for Women award (Grant RI8943103 to L.M.T.) and the National Institutes of Health (Grant GM 29222 to L.G.M.) for support. The NMR instrumentation was generously supported by NIH and NSF grants to Emory University. We also thank Mr. Srinivasan Mukundan for his assistance with molecular graphics.

(18) (a) Lippert, B. *Progress in Inorganic Chemistry*; Lippard, S. J., Ed.; John Wiley and Sons: New York, 1989; Vol. 37, p 23. (b) Bruhn, S. L.; Toney, J. H.; Lippard, S. J. *Progress in Inorganic Chemistry*; Lippard, S. J., Ed.; John Wiley and Sons: New York, 1990; Vol. 38, p 478.

(19) Sakurai, T.; Kobayashi, K.; Hasegawa, A.; Tsuboyama, S.; Tsuboyama, K. *Acta Crystallogr., Sect. B* 1982, 38, 1154.

(20) (a) Collins, A. D.; De Meester, P.; Goodgame, D. M. L.; Skapski, A. C. *Biochim. Biophys. Acta* 1975, 402, 1. (b) Chiang, C. C.; Epps, L. A.; Marzilli, L. G.; Kistenmacher, T. J. *Inorg. Chem.* 1979, 18, 791. (c) Sletten, E.; Thorstensen, B. *Acta Crystallogr., Sect. B* 1974, 30, 2438.

(21) Mukundan, S., Jr.; Xu, Y.; Zon, G.; Marzilli, L. G. *J. Am. Chem. Soc.* 1991, 113, 3021. For a consideration of appropriate conformations, see: Sherman, S. E.; Gibson, D.; Wang, A. H.-J.; Lippard, S. J. *J. Am. Chem. Soc.* 1988, 110, 7368.

## The Structure and Remarkable Stability of a Perypyridinium-Substituted Allyl Radical

Stephen G. DiMugno, Kenneth C. Waterman,  
Drew V. Speer, and Andrew Streitwieser\*

Department of Chemistry  
University of California, Berkeley  
Berkeley, California 94720

Received February 25, 1991

Revised Manuscript Received March 28, 1991

Allyl radical, the simplest example of a conjugated hydrocarbon possessing an unpaired electron, has been the subject of many theoretical and experimental studies. Recent multiconfiguration self-consistent field (MCSCF) calculations have shown that allyl radical has C<sub>2v</sub> symmetry,<sup>1</sup> in agreement with the experimental data from electron diffraction<sup>2</sup> and electron spin resonance.<sup>3</sup> Several examples of stable allyl radicals include 1,1,3,3-tetra-phenylallyl,<sup>4</sup> the polycrystalline 1,3-bis(diphenylene)-2-(*p*-chlorophenyl)allyl<sup>5</sup> and trifluoromethyl-substituted allyl radicals.<sup>6</sup> To our knowledge no crystal structure has been reported for an allylic radical. Here we report the preparation, properties, and

(1) Takada, T.; Dupuis, M. *J. Am. Chem. Soc.* 1983, 105, 1713. Kikuchi, O. *Chem. Phys. Lett.* 1980, 72, 487. Olivella, S.; Sole, A.; Bofill, J. M. *J. Am. Chem. Soc.* 1990, 112, 2160. Szalay, P. G.; Csaszar, A. G.; Fogarasi, G.; Karpfen, A.; Lischka, H. *J. Chem. Phys.* 1990, 93, 1246. Fjogstad, E.; Ystanes, M. *Spectrochim. Acta* 1990, 46A, 47.

(2) Vajda, E.; Tremmel, J.; Rozsondai, B.; Hargittai, E.; Maltsev, A. K.; Kagramanov, N. D.; Nefedov, O. M. *J. Am. Chem. Soc.* 1986, 108, 4352.

(3) Fessenden, R. W.; Schuler, R. H. *J. Chem. Phys.* 1963, 39, 2147. Sustman, R. In *Substituent Effects in Radical Chemistry*; Vieh, H. G., et al., Eds.; D. Reidel: Dordrecht, 1986.

(4) Watanabe, K.; Yamauchi, J.; Ohya-Nishiguchi, H.; Deguchi, Y.; Takaki, H. *Bull. Chem. Soc. Jpn.* 1972, 45, 371. Ziegler, K.; Bremer, G.; Thiel, F.; Thielman, F. *Justus Liebig's Ann. Chem.* 1923, 434, 34.

(5) Yamauchi, J.; Takeda, K.; Inoue, M. *Chem. Lett.* 1990, 9, 1551. Yamauchi, J. *J. Chem. Phys.* 1977, 67, 2850. Uchino, K.; Yamauchi, J.; Ohya-Nishiguchi, H.; Deguchi, Y. *Bull. Chem. Soc. Jpn.* 1974, 45, 285.

(6) Yamauchi, J.; Adachi, K.; Deguchi, Y. *J. Phys. Chem.* 1973, 35, 443. (6) Smart, B. E., private communication.

(14) Lu, Z.; Shorter, A. L.; Lin, I.; Dunaway-Mariano, D. *Inorg. Chem.* 1988, 27, 413.

(15) Mark, V.; Dungan, C. H.; Crutchfield, M. M.; van Wagner, R. In <sup>31</sup>P Nuclear Magnetic Resonance; Grayson, M., Griffith, E., Eds.; Wiley-Interscience: New York, 1967; p 227.

(16) Redfield, A. G.; Kuntz, A. D.; Ralph, E. K. *J. Magn. Reson.* 1978, 29, 433. Redfield, A. G.; Gupta, R. K. *J. Chem. Phys.* 1971, 54, 1418. Redfield, A. G.; Gupta, R. K. *Advances in Magnetic Resonance*; Waugh, J. S., Ed.; Academic Press: New York, 1971; Vol. 5, p 81.

(17) Diji, D.; Chottard, J.-C.; Girault, J.-P.; Reedijk, J. *Eur. J. Biochem.* 1989, 179, 333.

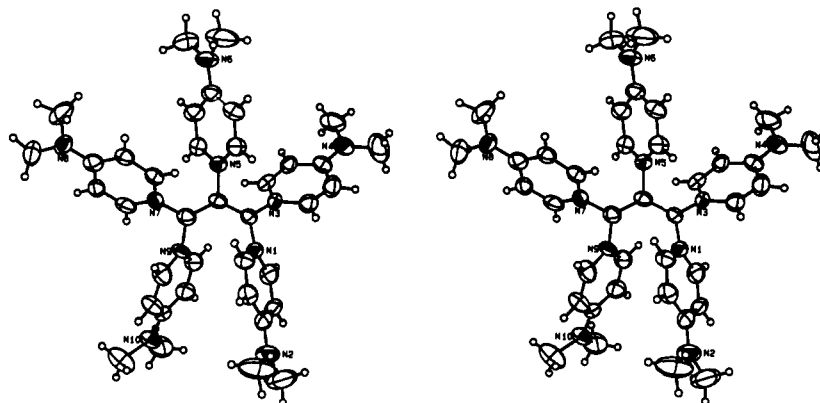
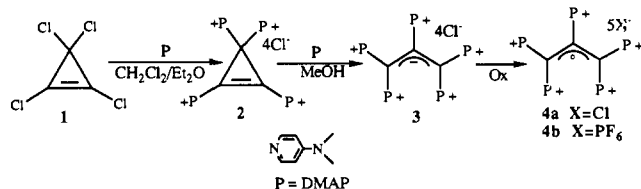


**Figure 1.** X-ray crystal structure of **4b** in which the ellipsoids are scaled to represent the 75% probability surface. The  $\text{PF}_6^-$  gegenions and the water molecules are removed for clarity.

#### Scheme I



X-ray crystal structure of a stable perpyridinium-substituted pentacationic allyl radical salt.

Recently, we reported the reaction of tetrachlorocyclopropene (**1**)<sup>7</sup> with 4-(dimethylamino)pyridine (DMAP) to give the 1,2,3-tetrakis(4-(dimethylamino)pyridinium-1-yl)cyclopropenyl tetrachloride (**2**) and further reaction with DMAP to give the highly stabilized allyl anion, 1,1,2,3,3-pentakis(4-(dimethylamino)pyridinium-1-yl)allyl tetrachloride (**3**)<sup>8,9</sup> (Scheme I).

Oxidation of **3** gave the corresponding 1,1,2,3,3-pentakis(4-(dimethylamino)pyridinium-1-yl)allyl radical pentachloride (**4a**). Cyclic voltammetry (CV) showed the oxidation to be a reversible process in aqueous solutions. The oxidation potential of the anion is +0.44 V vs the saturated calomel electrode, and the peak-to-peak separation is 60 mV. The electrochemistry is independent of the presence of dissolved oxygen.

Chemical oxidations have been carried out with chlorine, silver ion, and bromine. Chlorine gas bubbled through an aqueous solution of **3** produced an immediate color change from deep red to dark brown. Treatment of this solution with sodium bisulfite regenerated **3**, with the corresponding return of the deep red color. <sup>1</sup>H NMR experiments on the reduced solutions revealed that large excesses of chlorine gas led to substantial decomposition, but after use of a slight excess, **3** could be almost quantitatively regenerated. The use of NaOCl produced rapid decomposition; the radical is sensitive to hydroxide ion. Aqueous NaPF<sub>6</sub> added to solutions of the **4a** generated by chlorine oxidation gave a black precipitate, which was isolated by filtration and washed with water. Fractional recrystallization by slow evaporation of an acetonitrile/water solution over the course of 4 days yielded thin, intensely black plates of **4b** isolated as the pentakis(hexafluorophosphate) salt in 48% yield. Crystals grown in this manner were unsuitable for X-ray diffraction, but adequate for subsequent characterization.

Crystals of **4b** showed no sign of decomposition after months in air. Powdered samples of the hygroscopic salt **4a** decomposed after a few days on the bench top. The ESR spectrum of **4b** in acetonitrile showed a single, broad, featureless absorption with  $g = 2$ . The ESR spectrum of crystalline **4b** was significantly sharper than that obtained in solution, but the  $g$  value was un-

changed. Similar ESR results were obtained for **4a** in water or DMF solution. The UV-visible spectrum of **4b** in acetonitrile showed low-energy absorptions at  $\lambda_{\text{max}}$  (log  $\epsilon$ ) 696 (3.55), 606 (3.60), 500 (4.26), and 424 nm (4.42). Presumably these long-wavelength signals are due to transitions into and out of the singly occupied molecular orbital. The spectrum of **4b** also contains strong absorptions at 298 nm (4.76) and 330 nm (4.64) due to the pyridinium moieties. The UV-visible spectrum of **4a** in water is essentially identical with that obtained for **4b** in acetonitrile.

After numerous attempts, single crystals of **4** suitable for X-ray diffraction were obtained as follows: compound **3** was ion-exchanged to the tetrakis(hexafluorophosphate) salt and dissolved in acetonitrile. This solution was treated with a gross excess (10 equiv) of bromine. The solution was stirred for 1 h, and the solvent and excess bromine were removed in vacuo. The resultant black solid was fractionally recrystallized as above, and three types of crystals were isolated: needles, thin plates, and blocky polyhedra. To our surprise, only the needles showed any bromine content by analysis. The structure was elucidated from the diffraction on the polyhedral crystals.<sup>10</sup> The structure consists of parallel molecules of **4b**, the  $\text{PF}_6^-$  counterions, and molecules of water packed in the unit cell. There are five  $\text{PF}_6^-$  counterions and four water molecules per allyl molecule. Figure 1 shows an ORTEP plot of **4b**. The central bond angle C1–C2–C3 is 126.2 (7)°, and the bond lengths C1–C2 and C2–C3 are 1.38 (1) Å. The values from electron diffraction data for allyl radical are 124.6 (34)° and 1.428 (13) Å, respectively.<sup>2</sup> The values from MCSCF calculations are 124.3° and 1.388 Å, respectively.<sup>1</sup> The two terminal N–C–N planes are twisted with respect to the central C–C–C plane by 28° and 17°. Within the pyridinium moieties there is significant localization of the bonds. The average  $\text{C}_\gamma$ –NME<sub>2</sub> bond distance is 1.317 [7] Å.<sup>11</sup> Other average distances are N–C<sub>α</sub> = 1.370 [14] Å, C<sub>α</sub>–C<sub>β</sub> = 1.349 [9] Å, and C<sub>β</sub>–C<sub>γ</sub> = 1.419 [12] Å. This delocalization of charge into the DMAP rings has also been seen in other crystal structures.<sup>12</sup>

(10) Empirical formula,  $\text{P}_5\text{F}_{30}\text{O}_4\text{N}_{10}\text{C}_{38}\text{H}_{58}$ ; formula weight = 1443.8 amu; crystal parameters at  $T = -102^\circ\text{C}$ , triclinic unit cell, space group  $P1$ ,  $a = 13.717$  (3) Å,  $b = 14.308$  (2) Å,  $c = 17.829$  (6) Å,  $\alpha = 71.36$  (2)°,  $\beta = 80.24$  (2)°,  $\gamma = 61.431$  (16)°,  $V = 2911.2$  (11) Å<sup>3</sup>,  $Z = 2$ ,  $d(\text{calcd}) = 1.65$  g cm<sup>-3</sup>,  $\mu(\text{calcd}) = 2.9$  cm<sup>-1</sup>; radiation, Mo  $K\alpha$  ( $\lambda = 0.71073$  Å); the crystal was mounted on a glass fiber by using Paratone N hydrocarbon oil and transferred to an Enraf-Nonius CAD-4 diffractometer; monochromator, highly-oriented graphite ( $2\theta = 12.2$ ); detector, crystal scintillation counter, with PHA; reflections measured,  $h, \pm k, \pm l$ ;  $2\theta$  range,  $3^\circ \rightarrow 45^\circ$ ; scan type,  $\theta$ - $2\theta$ ; scan width,  $\delta\theta = 0.80 + 0.35 \tan(\theta)$ ; scan speed, 5.50 ( $\theta$ , deg/min); background, measured over  $0.25(\delta\theta)$  added to each end of the scan; vertical aperture = 4.0 mm, horizontal aperture =  $2.0 + 1.0 \tan \theta$  mm; number of reflections collected, 7586; number of unique reflections, 7586. The structure was solved by direct methods (MULTAN) in space group  $P1$  and refined via standard least-squares and Fourier techniques. No significant crystal decay was observed. The final residuals for 792 variables refined against the 5145 accepted data for which  $F_2 > 2\sum(F_2)$  were  $R = 8.5\%$ ,  $wR = 9.1\%$ , and  $\text{GOF} = 2.53$ . The  $R$  value for all data was 13.1%. The relatively large  $R$  values are principally due to the large amount of thermal motion associated with the  $\text{PF}_6^-$  gegenions.

(11) Where the  $[nn]$  is the standard deviation based on scatter of measurements.

(7) Tobey, S. W.; West, R. *J. Am. Chem. Soc.* **1966**, *88*, 2478–2480, 2481–2494.

(8) Waterman, K. C.; Streitwieser, A., Jr. *J. Am. Chem. Soc.* **1984**, *106*, 3874.

(9) Waterman, K. C.; Speer, D. V.; Streitwieser, A., Jr.; Look, G. C.; Nguyen, K. O.; Stack, J. G. *J. Org. Chem.* **1988**, *53*, 583–588.

**Acknowledgment.** This work was supported in part by National Science Foundation Grant DMR-8719302 and the Committee on Research, UCB. We also thank Dr. Fred Hollander for solving the crystal structure of **4b**.

**Supplementary Material Available:** Tables of atomic coordinates, intramolecular distances, intramolecular angles, torsion angles, anisotropic thermal parameters, and root-mean-square amplitudes of anisotropic displacement and a stereo figure for **4b** (17 pages). Ordering information is given on any current masthead page.

(12) Koch, A. S.; Waterman, K. C.; Banks, K.; Streitwieser, A. *J. Org. Chem.* **1990**, *55*, 6166. Speer, D. V.; Konigs, M.; Feng, A. S. F.; Streitwieser, A., manuscript in preparation.

## Nitrous Acid Cross-Links Duplex DNA Fragments through Deoxyguanosine Residues at the Sequence 5'-CG

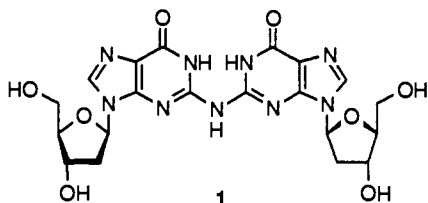
James J. Kirchner and Paul B. Hopkins\*

Department of Chemistry, University of Washington  
Seattle, Washington 98195

Received January 15, 1991

Defining the impact of nitrates, nitrites, and *N*-nitroso compounds on human health is important, given dietary and environmental exposure to these substances.<sup>1,2</sup> Sodium nitrite, for example, is a common additive to cured meats, contributing to their characteristic color and flavor, as well as protecting consumers against botulism.<sup>1-3</sup> Of several mechanisms suggested to account for the *in vitro* mutagenicity of nitrous acid,<sup>4</sup> one involves the creation of DNA interstrand cross-links.<sup>5</sup> Thus, in addition to providing insights into the chemical reactivity of duplex DNA, this reaction may be of biochemical significance. We report herein that treatment of duplex DNA fragments with nitrous acid forms thermally stable and base-stable interstrand cross-links preferentially through deoxyguanosine residues at the nucleotide sequences 5'-CG and 5'-GC, with a preference for the former.

Compound **1** is isolated on enzymatic hydrolysis of nitrous acid treated DNA and is a candidate for the nucleus of heat- and base-stable cross-links.<sup>6</sup> This suggests that spatially proximal



deoxyguanosine residues on opposite strands might be cross-linked.

(1) Committee on Nitrite and Alternative Curing Agents in Food. *The Health Effects of Nitrate, Nitrite, and N-Nitroso Compounds*; National Academy Press: Washington, DC 1981.

(2) WHO Task Group on Environmental Health Criteria for Nitrates, Nitrites, and N-Nitroso Compounds. *Environmental Health Criteria 5, Nitrates, Nitrites, and N-Nitroso Compounds*; World Health Organization: Geneva, 1978.

(3) Furia, T. E., Ed. *Handbook of Food Additives*, 2nd ed.; CRC Press: Cleveland, 1972; pp 150-155.

(4) Zimmerman, B. K. *Mutat. Res.* **1977**, *39*, 127.

(5) (a) Guideschek, E. P. *Proc. Natl. Acad. Sci. U.S.A.* **1961**, *47*, 950. (b) Becker, E. R.; Zimmerman, B. K.; Guideschek, E. P. *J. Mol. Biol.* **1964**, *8*, 377. (c) Burnotte, J.; Verly, W. G. *J. Biol. Chem.* **1971**, *246*, 5914.

(6) (a) Shapiro, R.; Dubelman, S.; Feinberg, A. M.; Crain, P. F.; McCloskey, J. A. *J. Am. Chem. Soc.* **1977**, *99*, 302. (b) Dubelman, S.; Shapiro, R. *Nucleic Acids Res.* **1977**, *4*, 1815.

To test this prediction, seven radiolabeled DNA duplexes<sup>7</sup> I-VII, 5'-d[AAATATAAT(N<sub>4</sub>)ATTAT], N<sub>4</sub> = AGCT (I), ACGT (II), TGCA (III), TCGA (IV), GGCC (V), CCGG (VI), and TATA (VII), in pH 4.5 sodium acetate (0.3 M) at 25 °C were treated with 0.5 M sodium nitrite for 1.5 h. DNA was isolated by ethanol precipitation and was evaluated by denaturing polyacrylamide gel electrophoresis (DPAGE). All experiments returned predominantly single stranded (high-mobility) DNA. The yields (Cerenkov counting) of the least mobile,<sup>9</sup> interstrand cross-linked products were as follows: AGCT (I, 3.2%), CCGG (VI, 2.4%) > ACGT (II, 0.76%), TCGA (IV, 0.62%) > TGCA (III, 0.16%), GGCC (V, 0.09%) >> TATA (VII, <0.05%).

The cross-linked DNAs ACGT (II), TGCA (III), TCGA (IV), GGCC (V), and CCGG (VI) were stable to base (1 M aqueous piperidine, 90 °C, 0.5 h). For cross-linked DNAs ACGT (II), TCGA (IV), and CCGG (VI), analyses of the cross-link position at nucleotide resolution<sup>8,10-12</sup> revealed a single dG to dG cross-link at the central 5'-CG sequence (for example, Figure 1), consistent with **1** as the nucleus of the cross-links. Similar analyses of cross-linked TGCA (III) and GGCC (V) indicated heterogeneity of cross-link position,<sup>8</sup> but in both cases linkage was predominantly dG to dG at 5'-GC. In contrast, the cross-link formed by the most efficiently cross-linked DNA, AGCT (I), was thermally labile (H<sub>2</sub>O, 90 °C), reverting under these conditions predominantly to single strands (gel mobility assay).<sup>13</sup> It is thus likely that this cross-link is structurally distinct and its formation mechanistically distinct from those at the other 5'-CG and 5'-GC sequences.

Among those DNAs that form thermally stable and base-stable dG to dG linkages (as in **1**), there exists a preference for cross-linking at the nucleotide sequence 5'-CG relative to 5'-GC [4-fold in TCGA (IV) vs TGCA (III); 25-fold in CCGG (VI) vs GGCC (V)]. The mechanistic origin of this preference is unknown, but differences in ground-state DNA structure may be relevant. A plausible mechanism for cross-linking involves sequential diazotization of N2 of one dG residue, nucleophilic attack by N2 of the neighboring dG residue on C2 of the diazotized residue, and loss of N<sub>2</sub>.<sup>6</sup> The sequence 5'-CG in the B conformation<sup>14</sup> is structurally matched to the addition step (Figure 2), with the putative reactive centers being in van der Waals contact. The isomeric sequence 5'-GC requires a 3-Å sliding of the base pairs relative to one another to bring these reactive centers into contact. Achievement of the strand-linking transition state with only slight conformational reorganization at the sequence 5'-CG might correspond to a lower transition-state energy. This is obviously not the whole story, however, given flanking sequence effects on cross-linking efficiency.<sup>15</sup>

Nitrous acid thus cross-links deoxyguanosine residues in duplex DNA with a preference for the sequence 5'-CG, supporting **1** as the nucleus of nitrous acid promoted, heat- and base-stable DNA interstrand cross-links. Knowledge of this sequence preference

(7) DNA was synthesized, purified, and radiolabeled as previously described.<sup>8</sup>

(8) (a) Millard, J. T.; Weidner, M. F.; Raucher, S.; Hopkins, P. B. *J. Am. Chem. Soc.* **1990**, *112*, 3637. (b) Weidner, M. F.; Sigurdsson, S. Th.; Hopkins, P. B. *Biochemistry* **1990**, *29*, 9225.

(9) All DNAs tested returned several interstrand cross-linked products (distinct DPAGE bands); only the least mobile band ever exceeded 0.1% yield. DPAGE mobility of cross-linked DNA is a function of cross-link position, with cross-links farthest from the duplex termini having lowest mobility.<sup>10</sup>

(10) Millard, J. T.; Weidner, M. F.; Kirchner, J. J.; Ribeiro, S.; Hopkins, P. B. *Nucleic Acids Res.*, in press.

(11) Weidner, M. F.; Millard, J. T.; Hopkins, P. B. *J. Am. Chem. Soc.* **1989**, *111*, 9270.

(12) Hopkins, P. B.; Millard, J. T.; Woo, J.; Weidner, M. F.; Kirchner, J. J.; Sigurdsson, S. Th.; Raucher, S. *Tetrahedron* **1991**, *47*, 2475.

(13) A byproduct of reversion to single strands has DPAGE mobility consistent with scission at the bold T of AGCT (I), suggesting partial cross-linking dG to dT at 5'-AG.

(14) Arnott, S.; Campbell-Smith, P.; Chandrasekharan, P. In *CRC Handbook of Biochemistry*; CRC Press: Boca Raton, FL, 1976; Vol. 2, pp 411-422.

(15) Other explanations, including preferential diazotization at 5'-CG or preferential hydrolysis of a diazotized dG at 5'-GC, are currently under investigation.